Int J Theor Phys (2007) 46: 2816–2828
DOI 10.1007/s10773-007-9393-3

Superposition of the Finite Dimensional Pair Coherent State and Some Nonclassical Properties

E.M. Khalil

Published online: 15 May 2007

Abstract In this communication we study a superposition of two finite dimensional pair coherent states. We show that such states possess inherent nonclassical properties such as sub-Poissonian distribution, anti-correlation between the two-mode and violation of Cauchy–Schwarz inequalities. The s-parameterized characteristic function (CF) is considered. Furthermore, the phase distribution in the framework of Pegg and Barnett formalism, W-function and Q-function are discussed. General conclusions reached are illustrated by numerical results.

1 Introduction

The study of the nonclassical states of light has recently attracted renewed attention because of the key role they may play, beyond the traditional realm of quantum optics, in research fields of great current interest, such as laser pulsed atoms and molecules [1]; Bose–Einstein condensation and atom lasers [2, 3]; and quantum information theory [4, 5]. The simplest archetype examples of nonclassical states are of course number states, whose experimental realization is however difficult to achieve. Moreover they share very few of the coherence properties that would be desirable both in practical implementations and in fundamental experiments. The most important experimentally accessible nonclassical states are the two-photon squeezed states [6–9]. They are Gaussian, exhibit several important coherence properties, and can be obtained by suitably generalizing the notion of coherent states [8]. The coherent state has become a useful and necessary tool for treating ideal boson fields subjected to external pumping sources. Although any quantum state can be described in terms of the coherent states due to their resolution of unity, the coherent states themselves are classical states in which nonclassical effects such as antibunching, squeezing, etc. cannot occur. A generalized class of the conventional coherent state called the nonlinear coherent states or the f-coherent state [11, 12] has been constructed.

E.M. Khalil (✉)
Mathematics Department, Faculty of Science, Al-Azher University, Nassr City 11884, Cairo, Egypt
e-mail: eiedkhalil@yahoo.com

On the other hand, pair coherent states (PCS) are regarded as an important type of correlated two-mode states, which possess prominent nonclassical properties. Such states denoted by $|\xi, q\rangle$ are eigenstates of the pair operator $(\hat{a}\hat{b})$ and the number difference $(\hat{n}_a - \hat{n}_b)$ where $\hat{a}$ and $\hat{b}$ are the annihilation operators of the field modes and $\hat{n}_a = \hat{a}^\dagger\hat{a}$ and $\hat{n}_b = \hat{b}^\dagger\hat{b}$. These states satisfy

$$\hat{a}\hat{b}|\xi, q\rangle = \xi|\xi, q\rangle \quad \text{and} \quad (\hat{n}_a - \hat{n}_b)|\xi, q\rangle = q|\xi, q\rangle. \tag{1}$$

The experimental realization of such nonclassical states is a practical importance. Agarwal [13, 14] suggested that the optical (PCS) can be generated via the competition of 4-wave mixing and two-photon absorption in a nonlinear medium. Another scheme has been suggested for generating vibrational pair coherent states via the motion of a trapped ion in a two-dimensional trap [15].

An ion confined in an electromagnetic trap can be regarded as a particle with quantized center-of-mass motion in a harmonic potential. Exciting or deexciting the internal atomic states of the trapped ion by a classical laser driving field changes the external states of the ion motion, as atomic stimulated absorption and emission processes are always accompanied by momentum exchange of the laser field with the ion. If the vibrational amplitude of the ion is much smaller than the laser wavelength, i.e., in the Lamb–Dicke limit [16, 17], and the driving field is tuned to one of the vibrational side-bands of the atomic transition, then this model can be simplified to a form similar to the Jaynes–Cummings model (JCM) [18] in which the quantized radiation field is replaced by the quantized center-of-mass motion of the ion. As the coupling between the vibrational modes and the external environment is extremely weak, dissipative effects which are inevitable from cavity damping in the optical regime, can be significantly suppressed for the ion motion. This unique feature thus makes it possible to realize cavity QED experiments without using an optical cavity. Following this approach, nonclassical vibrational states of the trapped ions such as Fock [19, 20], squeezed [21] and Schrödinger cat states [22] have been proposed and observed [23].

On the other hand, the finite dimensional PCS has been studied recently by [24, 25] as the eigenstate of the pair operators $(\hat{a}^\dagger\hat{b} + \frac{\zeta^{q+1}(\hat{a}\hat{b}^\dagger)^q}{(q!)^2})$ and the sum of the photon number operators for the two modes $(\hat{Q} = \hat{n}_a + \hat{n}_b)$. namely:

$$\begin{aligned} \left(\hat{a}^\dagger\hat{b} + \frac{\zeta^{q+1}(\hat{a}\hat{b}^\dagger)^q}{(q!)^2}\right)|\zeta, q\rangle &= \zeta|\zeta, q\rangle, \\ \hat{Q}|\zeta, q\rangle &= q|\zeta, q\rangle, \end{aligned} \tag{2}$$

where the parameter ζ is a complex variable while the parameter q is an integer. The state takes the form,

$$|\zeta, q\rangle = N_q \sum_{n=0}^{q} \zeta^n \sqrt{\frac{(q-n)!}{q!n!}}|q-n, n\rangle, \tag{3}$$

in the two mode states $|n_a, n_b\rangle = |n_a\rangle \otimes |n_b\rangle$, where $|n_s\rangle$ is the Fock state for the mode s ($s = a$ or b) and the normalization constant N_q is given by

$$N_q = \left[\sum_{n=0}^{q} |\zeta|^{2n} \frac{(q-n)!}{q!n!}\right]^{\frac{-1}{2}} = ({}_1F_0(-q, -|\zeta|^2))^{\frac{-1}{2}}, \tag{4}$$

where ${}_1F_0$ is a generalized hypergeometric function. In the present communication we develop this idea and introduce a superposition of two finite dimensional PCS. The correlated two-mode states $|\zeta, q, \phi\rangle$ are defined as superposition of two finite dimensional state separated in phase by π.

$$|\zeta, q, \phi\rangle = N_\phi[|\zeta, q\rangle + \exp(i\phi)|-\zeta, q\rangle], \tag{5}$$

where the normalization constant N_ϕ is given by

$$N_\phi = \frac{1}{\sqrt{2}}\left[1 + N_q^2 \cos\phi \sum_{n=0}^{q}(-1)^n|\zeta|^{2n}\frac{(q-n)!}{q!n!}\right]^{-\frac{1}{2}}. \tag{6}$$

It is easy to verify that the states $|\zeta, q, \phi\rangle$ are eigenstates of the operator $(\hat{a}^\dagger\hat{b} + \frac{\zeta^{q+1}(\hat{a}\hat{b}^\dagger)^q}{(q!)^2})^2$ with eigenvalue ζ^2. In this contribution we focus on the two special cases of ϕ (namely $\phi = 0$ and π), the general form can be rewritten as follows:

$$\begin{aligned} |\zeta, q\rangle_j &= N_{q,j}^2 \sum_{n=0}^{[\frac{q-j}{2}]} \zeta^{2n+j}\sqrt{\frac{(q-2n-j)!}{q!(2n+j)!}}|q-2n-j, 2n+j\rangle, \\ N_{q,j}^{-2} &= \sum_{n=0}^{[\frac{q-j}{2}]}|\zeta|^{4n+2j}\frac{(q-2n-j)!}{q!(2n+j)!}, \quad j = 0, 1. \end{aligned} \tag{7}$$

Now we discuss some statistical properties of these correlated two mode states of (7). The results that we are going to present stem from a new approach to the superposing of the finite dimensional state. Subsequently we shall examine the sub-Poissonian distribution, The behavior of the phase distribution in the framework of Pegg and Barnett formalism, the Wigner function the Q-function of the state (7) are discussed.

2 Sub-Poissonian Distribution

We devote in the present section to consider an example of the nonclassical effects that is the phenomenon of sub-Poissonian distribution. This phenomenon can be measured by photon detectors based on photoelectric effect. The importance of the study comes up as a result of several applications, e.g. in the gravitational wave detector and quantum nondemolition measurement, which can be generated in semiconductor lasers [26] and in the microwave region using masers operating in the microscopic regime [27]. It is well known that, sub-Poissonian statistics is characterized by the fact that the variance of the photon number $\langle(\Delta\hat{n}_i(t))^2\rangle$ is less than the average photon number $\langle\hat{a}_i^\dagger(t)\hat{a}_i(t)\rangle = \langle\hat{n}_i(t)\rangle$. This can be expressed by means of the normalized second-order correlation function [28] as follows.

$$g_z^{(2)}(\zeta) = \frac{{}_j\langle\zeta, q|\hat{n}_z(\hat{n}_z - 1)|\zeta, q\rangle_j}{{}_j\langle\zeta, q|\hat{n}_z|\zeta, q\rangle_j^2}, \quad \forall z = a, b \tag{8}$$

where

$$
\begin{aligned}
&{}_j\langle\zeta,q|\hat{n}_a(\hat{n}_a-1)|\zeta,q\rangle_j \\
&\quad=N_{q,j}^2\sum_{n=0}^{[\frac{q-j}{2}]}\frac{|\zeta|^{4n+2j}(q-2n-j)!}{q!(2n+j)!}(q-2n-j)(q-2n-j-1), \\
&{}_j\langle\zeta,q|\hat{n}_b(\hat{n}_b-1)|\zeta,q\rangle_j \\
&\quad=N_{q,j}^2\sum_{n=0}^{\frac{q-j}{2}}\frac{|\zeta|^{4n+2j}(q-2n-j)!}{q!(2n+j)!}(2n+j)(2n+j-1),
\end{aligned}
\tag{9}
$$

and

$$
\begin{aligned}
{}_j\langle\zeta,q|\hat{n}_a|\zeta,q\rangle_j &= N_{q,j}^2\sum_{n=0}^{[\frac{q-j}{2}]}\frac{|\zeta|^{4n+2j}(q-2n-j)!}{q!(2n+j)!}(q-2n-j), \\
{}_j\langle\zeta,q|\hat{n}_b|\zeta,q\rangle_j &= N_{q,j}^2\sum_{n=0}^{[\frac{q-j}{2}]}\frac{|\zeta|^{4n+2j}(q-2n-j)!}{q!(2n+j)!}(2n+j).
\end{aligned}
\tag{10}
$$

The function $g_z^{(2)}(\zeta)$ given by (8) for the mode z serves as a measure of the deviation from the Poissonian distribution that corresponds to coherent states with $g_z^{(2)}(\zeta)=1$. If $g_z^{(2)}(\zeta)<1$ (>1), the distribution is called sub (super-)Poissonian, if $g_z^{(2)}(\zeta)=2$ the distribution is called thermal and when $g_z^{(2)}(\zeta)>2$ it is called super-thermal.

In Fig. 1(a), the second-order correlation function $g_a^{(2)}(\zeta)$ given by (8) for q taking odd numbers is plotted against $|\zeta|$ for $q=3,5,7$ there exist two cases. The first case when we take $j=0$, this figure exhibits the very striking quantum nature of the generated field. For the first mode, we find that the distribution function starts to be sub-Poissonian $g_a^{(2)}(0)<1$ at small values of $|\zeta|$ which is started from $\frac{q-1}{q}$, but for increasing of the parameter q the function $g_a^{(2)}(\zeta)$ reaches a super-Poissonian distribution ($g_a^{(2)}(\zeta)>1$) as appearing in Fig. 1(a). For the second mode at some value of $|\zeta|$ the state with $j=0$ becomes super-thermal ($g_b^{(2)}(0)>2$) while the state with higher values of ζ the distribution becomes sub-Poissonian. Thus when we take the limits as $\zeta\to\infty$ we get these limit $g_b^{(2)}(\zeta)=\frac{q}{q-1}$ see Fig. 1(b).

The second case when we take $j=1$. In this case we find larger changes occurring in the shape of the curve for the function $g_a^{(2)}(\zeta)$. For the first mode the function $g_a^{(2)}(\zeta)$

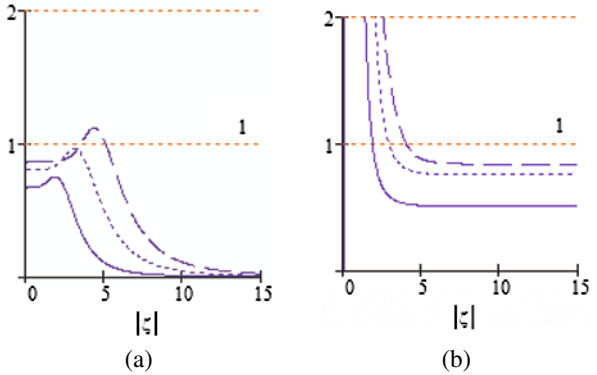

Fig. 1 The sub-Poissonian distribution as a function of $|\zeta|$, $j=0$. **a** For mode a, **b** for mode b, where the solid curve for $q=3$, the dotted curve for $q=5$ and the dashed curve for $q=7$

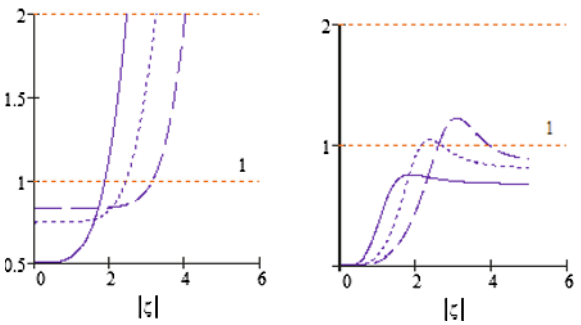

Fig. 2 Same as Fig. 1 but $j = 1$

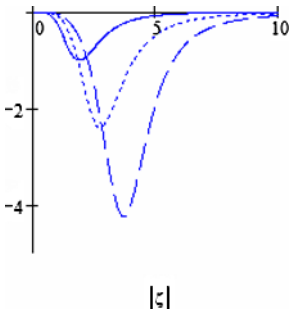

Fig. 3 The cross correlation between the two-mode as a function of $|\zeta|$, $j = 0$ where the solid curve for $q = 3$, the dotted curve for $q = 5$ and the dashed curve for $q = 7$

starts with sub-Poissonian distribution. For higher values of $|\zeta|$ the function $g_a^{(2)}(\zeta)$ becomes super-Poissonian and super-thermal as observed in Fig. 2(a). For the second mode the function $g_b^{(2)}(\zeta)$ starts from 0, by increasing of the parameter $|\zeta|$ the function reaches to super-Poissonian see Fig. 2(b). Increasing of $|\zeta|$ makes the distribution returns to sub-Poissonian distribution. The limits as $\zeta \to \infty$ equal $g_b^{(2)}(\zeta) = \frac{q-1}{q}$.

When q takes even numbers, for the first and the second modes when $(j = 0, 1)$ the behavior is the same as the above case when $(j = 1, 0)$ respectively, for the other parameters fixed.

The cross correlation between the two-mode is given by

$$\Delta_{\text{cross}}(\zeta) = {}_j\langle\zeta, q|\hat{n}_a\hat{n}_b|\zeta, q\rangle_j - {}_j\langle\zeta, q|\hat{n}_a|\zeta, q\rangle_{jj}\langle\zeta, q|\hat{n}_b|\zeta, q\rangle_j.$$

If Δ_{cross} is a positive quantity, this means that the modes are correlated, while anti-correlation amongst the modes occurs when Δ_{cross} is negative values. In Fig. 3 the cross correlation function $\Delta_{\text{cross}}(\zeta)$ is plotted against $|\zeta|$ for $q = 3, 5, 7$. From the figure the function $\Delta_{\text{cross}}(\zeta)$ is negative and the nonclassicality behavior is demonstrated by increase of the parameter q.

3 Cauchy–Schwarz Inequality Violation

The Cauchy–Schwarz inequality [29] is defined as

$${}_j\langle\zeta, q|\hat{n}_a(\hat{n}_a - 1)|\zeta, q\rangle_j\, {}_j\langle\zeta, q|\hat{n}_b(\hat{n}_b - 1)|\zeta, q\rangle_j \geq {}_j\langle\zeta, q|\hat{n}_a\hat{n}_b|\zeta, q, \rangle_j^2. \tag{11}$$

We shall examine the scaled Cauchy–Schwarz inequalities in the superposition of the finite dimensional PCS which determined by

$$F_{ab}(\zeta) = \frac{{}_j\langle\zeta, q|\hat{n}_a(\hat{n}_a - 1)|\zeta, q\rangle_j \, {}_j\langle\zeta, q|\hat{n}_b(\hat{n}_b - 1)|\zeta, q\rangle_j}{{}_j\langle\zeta, q|\hat{n}_a\hat{n}_b|\zeta, q, \rangle_j^2}. \tag{12}$$

The inequality (11) is violated if the function F_{ab} is less than unity. For that purpose we need to calculate the expectation values appearing in (12). Those in the numerator were already known from (9) and those in the denominator are calculated to be generally for $j = 0, 1$.

$${}_j\langle\zeta, q|\hat{n}_a\hat{n}_b|\zeta, q\rangle_j = N_{q,j}^2 \sum_{n=0}^{[\frac{q-j}{2}]} \frac{|\zeta|^{4n+2j}(q-2n-j)!}{q!(2n+j)!}(q-2n-j)(2n+j). \tag{13}$$

The Cauchy–Schwarz inequality for the finite dimensional pair coherent state is clearly seen in Fig. 4 for the two modes (a, b). Where $q = 3, 5, 7$ and for case $j = 0$, partial violation starting from non-zero for short interval of $|\zeta|$ and full violated after short interval (a partial violation means that $F_{23} > 1$ at small $|\zeta|$ and then becomes less than unity for large $|\zeta|$). As the parameter $|\zeta|$ increases the function $F_{ab}(\zeta)$ reaches zero as in Fig. 4(a). For $j = 1$ full violation starting from zero, after short interval the function $F_{ab}(\zeta)$ becomes partially violated as observed in Fig. 4(b). The second case when q takes even number namely $(q = 4, 6, 8)$. For $j = 0$ we see that all curves do not suffer violation and they never reach unity see Fig. 5(a). While $j = 1$ the function $F_{ab}(\zeta)$ shown full violation starting from zero,

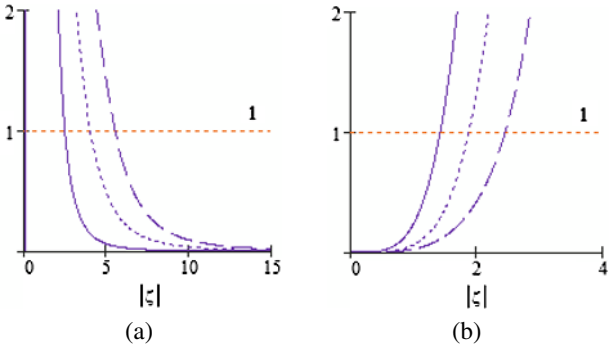

Fig. 4 F_{ab} as a function of $|\zeta|$, **a** for fixed $j = 0$ and the solid curve for $q = 3$, the dotted curve for $q = 5$ and the dashed curve for $q = 7$, **b** same as (**a**) but $j = 0$

Fig. 5 Same as Fig. 3 but the solid curve for $q = 4$, the dotted curve for $q = 6$ and the dashed curve for $q = 8$

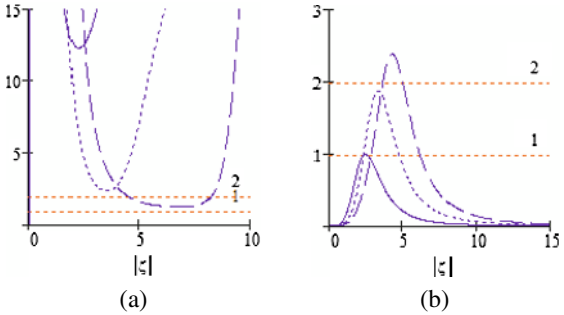

as the parameter $|\zeta|$ progresses the function $F_{ab}(\zeta)$ shows partial variation. After short interval the behavior returns to full violation and the function $F_{ab}(\zeta)$ reaches zero as observed in Fig. 5(b). The violation is stronger (weaker) at small $|\zeta|$ (large $|\zeta|$)-region. However, the variation depends on the parameter ζ for small values of q the function $F_{ab}(\zeta)$ almost less than unity. But for larger values of q the function $F_{ab}(\zeta)$ shows partial violation.

4 Phase Properties

In this section we shall discuss the phase distribution for the present states. For this reason it is convenient to use the phase distribution formalism introduced by Barnett and Pegg [24, 25, 28, 30–35]. It is well known that the phase operator is defined as the projection operator on a particular phase state multiplied by the corresponding value of the phase. Therefore one can find that the Pegg–Barnett phases distribution function $P_{\zeta,q}(\theta_1,\theta_2)$ is given by [33–35]:

$$P_{\zeta,q}(\theta_1,\theta_2)=\frac{|N_q|^2}{(2\pi)^2}\sum_{n,m}\zeta^{2n+j}\zeta^{*2m+j}\sqrt{\frac{(q-2n-j)!(q-2m-j)!}{q!(2n+j)!q!(2m+j)!}}$$
$$\times\exp[i[(q-2n-j)-(q-2m-j)]\theta_1+i(2n-2m)\theta_2]. \qquad (14)$$

Therefore the phases distribution function can be written as

$$P_{\zeta,q}(\theta_1,\theta_2)=\frac{|N_q|^2}{(2\pi)^2}\left|\sum_n\zeta^{2n+j}\sqrt{\frac{(q-2n-j)!}{q!(2n+j)!}}\exp[i2n\theta]\right|^2,\quad -\pi\le\theta\le\pi \qquad (15)$$

with $\theta=\theta_2-\theta_1$, which is normalized according to $\int_{-\pi}^{\pi}\int_{-\pi}^{\pi}P(\theta_1,\theta_2,\zeta)d\theta_1 d\theta_2=1$. Due to the correction between the two modes, the phase distribution depends on the difference between the phases of the modes. In the figures we plot $P_{\zeta,q}(\theta)$ against the angle $\theta=\theta_2-\theta_1$ for different values of the parameter q and $|\zeta|$.

Generally for very small (large) values of $|\zeta|$ the state (7) almost represents a Fock state and hence the information about the phase is lost. As $|\zeta|$ increases partial coherent phase states result and the phase distribution shows a thee-peak structure. These peaks is centered around $\theta=0$ and the distribution is symmetric around the central peak. For $q=3$, plotted

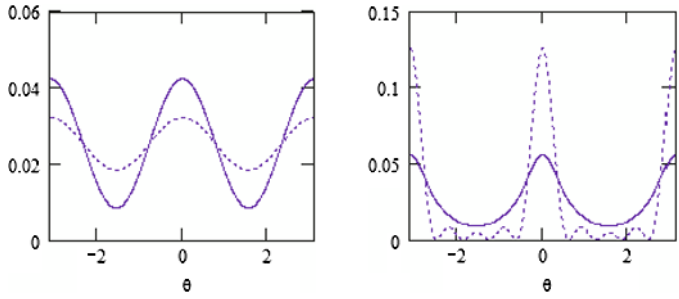

(a) (b)

Fig. 6 The phase distribution $P(\theta)$ as a function of θ and **a** $j=0$, the solid curve for $\zeta=3$ and the dotted curve for $\zeta=5$, **b** same as (**a**) but $j=1$

in Fig. 6(a), it is observed that $P_{\zeta,q}(\theta)$ starts at $P_{\zeta,q}(-\pi) = 0.042, 0.032$ when $|\zeta| = 3, 5$ respectively. The maxima for the distribution at $\theta = 0$ decrease by increasing $|\zeta| = 3$. In Fig. 6(b) we take a large value for the parameter q $(q = 10)$ and the same values of $|\zeta|$ (3, 5). We see that the function $P_{\zeta,q}(\theta)$ starts at $P(-\pi) = 0.056, (0.125)$ when $|\zeta| = 3, (5)$ respectively. The maxima for the distribution.at $\theta = 0$ by increasing the value of $|\zeta|$. In Fig. 6(b) we take larger values for the parameter q $(q = 10)$ and the same values of $|\zeta|$ (3, 5). We see that the function $P_{\zeta,q}(\theta)$ starts at $P_{\zeta,q}(\theta) = 0.056, (0.125)$ when $|\zeta| = 3, (5)$ respectively. The maxima of the phase distribution are increased by increasing of the parameter $|\zeta|$ (see Fig. 6(b)). However this increase turns to a decrease for larger values of $|\zeta|$. The maximum value for $P_{\zeta,q}(0)$ shifts to higher values of $|\zeta|$ as q increases.

5 s-Parameterized Quasiprobability Function

The QDF's for a quantum state of a physical system are useful tools for investigating the dynamical and statistical properties of a quantum mechanical system [36–54]. They include the Glauber–Sudarshan P-function [10, 38], the Wigner W-function [36, 37] and the Husimi Q -function [39, 40] which are closely related to the operator ordering in the mathematical description of a physical system.

The s-parameterized characteristic function (CF) is perhaps one of the most well-known important function in quantum optics, since it is the Fourier transformation of the s-parameterized QDF. The s-parameterized CF for a single-mode field is defined by [44–46]

$$C(\lambda, s) = \mathrm{Tr}[\hat{\rho}\hat{D}(\lambda)] \exp\left(\frac{s}{2}|\lambda|^2\right), \tag{16}$$

with $\hat{D}(\lambda)$ is the displacement operator given by $\hat{D}(\lambda) = \exp(\lambda\hat{a}^+ - \lambda^*\hat{a})$, and $\lambda = |\lambda|e^{i\theta}$. Here, s is ordering parameter where $s = (-1)$ 1 means (anti-)normal ordering and $s = 0$ is symmetrical or Weyl ordering [44–46].

The s-parameterized quasi-probability function is the Fourier transformation of the s-parameterized characteristic function

$$F(\beta, s) = \frac{1}{\pi^2}\int C(\lambda, s) \exp(\lambda^*\beta - \lambda\beta^*) d^2\lambda, \tag{17}$$

where the real parameter s defines the corresponding phase space distribution. It is well known that such a parameter is associated with the ordering of the field bosonic operators.

Since the finite dimensional PCS (7) is a two-mode state, thus the definitions (16), and (17) have to be extended to two-mode case. The s-parameterized CF for the two-mode states is defined as follows

$$C(\lambda_1, \lambda_2, s) = \mathrm{Tr}[\hat{\rho}\hat{D}(\lambda_1)\hat{D}(\lambda_2)] \exp\left\{\frac{s}{2}(|\lambda_1|^2 + |\lambda_2|^2)\right\}. \tag{18}$$

With the s-parameterized QDF for the two-mode case given by

$$F(\beta_1, \beta_2, s) = \left(\frac{1}{\pi^2}\right)^2 \iint C(\lambda_1, \lambda_2, s) \times \exp(\lambda_1^*\beta_1 + \lambda_2^*\beta_2 - \lambda_1\beta_1^* - \lambda_2\beta_2^*) d^2\lambda_1 d^2\lambda_2. \tag{19}$$

It is to be noted that formulae (18) and (19) are extensions of formulae (16) and (17) for CF and QDF of the single mode fields.

We consider a phase space QDF for our states. To begin the state (7) will be written in the form

$$|\zeta, q\rangle_B = \sum_{n=0}^{[\frac{q-j}{2}]} B_n(\zeta, q)|q-2n-j, 2n+j\rangle, \tag{20}$$

where

$$B_n(\zeta, q) = N_{q,j}^2\, \zeta^{2n+j} \sqrt{\frac{(q-2n-j)!}{q!(2n+j)!}}.$$

For the density operator $\hat{\rho} = |\zeta, q\rangle\langle q, \zeta|$ the s-parameterized CF has the two mode form. Using (20) for the state (7) in the formulae (18) and (19), we get

$$\begin{aligned} C(\lambda_1, \lambda_2, s) = \exp\left[\left\{-\frac{(1-s)}{2}\right\}(|\lambda_1|^2 + |\lambda_2|^2)\right] \\ \times \sum_{n=0}^{[\frac{q-j}{2}]}\sum_{m=0}^{[\frac{q-j}{2}]} B_n(\zeta, q) B_m^*(\zeta, q) \sqrt{\frac{(q-2n-j)!}{(q-2m-j)!}} \\ \times \sqrt{\frac{(2n+j)!}{(2m+j)!}} L_{q-2n-j}^{2n-2m}[|\lambda_1|^2] L_{2n+j}^{2m-2n}[|\lambda_2|^2], \end{aligned} \tag{21}$$

where $L_m^n(x)$ are associated Laguerre polynomials given by

$$L_m^n(x) = \sum_{r=0}^{m} \binom{m+n}{m-r} \frac{(-1)^r}{r!} x^r, \tag{22}$$

$$\begin{aligned} F(\beta_1, \beta_2, s) = N_{q,j}^2 \left(\frac{2}{\pi(1-s)}\right)^2 \exp\left[\frac{-2(|\beta_1|^2 + |\beta_2|^2)}{(1-s)}\right] \\ \times \sum_{n=0}^{[\frac{q-j}{2}]}\sum_{m=0}^{[\frac{q-j}{2}]} \zeta^{2n+j} \zeta^{*2m+j} \frac{(q-2n-j)!}{(2m+j)!} \\ \times \left(\frac{1+s}{(1-s)}\right)^q L_{q-2n-j}^{2n-2m}\left[\frac{4|\beta_1|^2}{(1-s^2)}\right] L_{2n+j}^{2m-2n}\left[\frac{4|\beta_2|^2}{(1-s^2)}\right]. \end{aligned} \tag{23}$$

Note that in (21) and (23) there exist two associated Laguerre polynomials. For negative values of $(m-n)$ or $(n-m)$ we are use the formula [55]

$$L_{n+\alpha}^{(-\alpha)}(z) = (-z)^\alpha \frac{n!}{(n+\alpha)!} L_n^{(\alpha)}(z).$$

For visualization let us confine ourselves to a subspace determined by $\alpha = \beta$ [56], we find that the s-parameterized QDF for our field states may be written in the following form:

$$F(\beta, s) = N_{q,j}^2 \left(\frac{2}{\pi(1-s)}\right)^2 \exp\left[\frac{-4(|\beta|^2)}{(1-s)}\right] \sum_{n=0}^{[\frac{q-j}{2}]} |\zeta|^{4n+2j} \frac{(q-2n-j)!}{(2n+j)!}$$

$$\times \left(\frac{1+s}{(1-s)}\right)^{q} L^{0}_{q-2n-j}\left[\frac{4|\beta|^2}{(1-s^2)}\right] L^{0}_{2n+j}\left[\frac{4|\beta|^2}{(1-s^2)}\right]. \tag{24}$$

This formula gives the exact analytical expressions for the s-parameterized QDF for the state (7). It is noted that, for the P-function, i.e., $s = 1$, special attention has to be paid in performing the limit $s \to 1$ [52, 53]. Originally the P function was introduced in an alternative way independently by Glauber and Sudershan [38]. Recently, Wünsche discussed the nonclassicality of states defined by nonpositivity of the P-function [52, 53]. However we shall not discuss this function here any further. Instead we concentrate on the other two quasi-probability functions namely Wigner and Q-functions.

In Fig. 7 we plot $W(\beta)$, i.e., $s = 0$ in (24) for $j = 1, \zeta = 5$, and $q = 4$ and 5. It is clear that (for q odd) the Wigner function has negative peak at the origin observed and oscillatory regime around the main peak. The non-classicality effect is more pronounced when q is

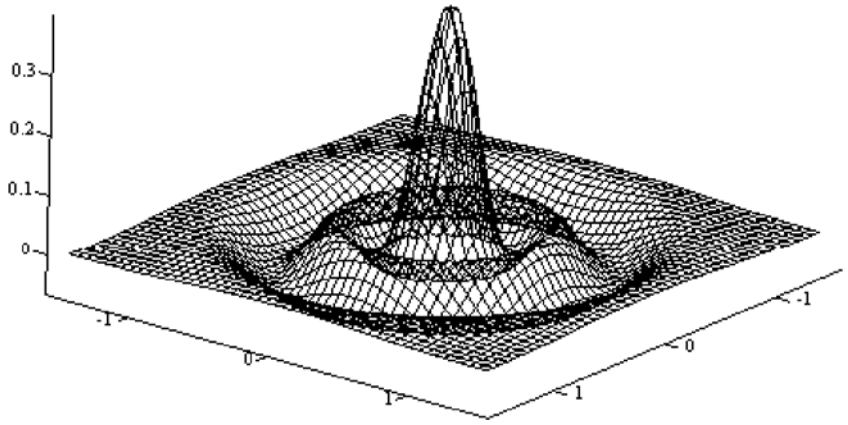

(a)

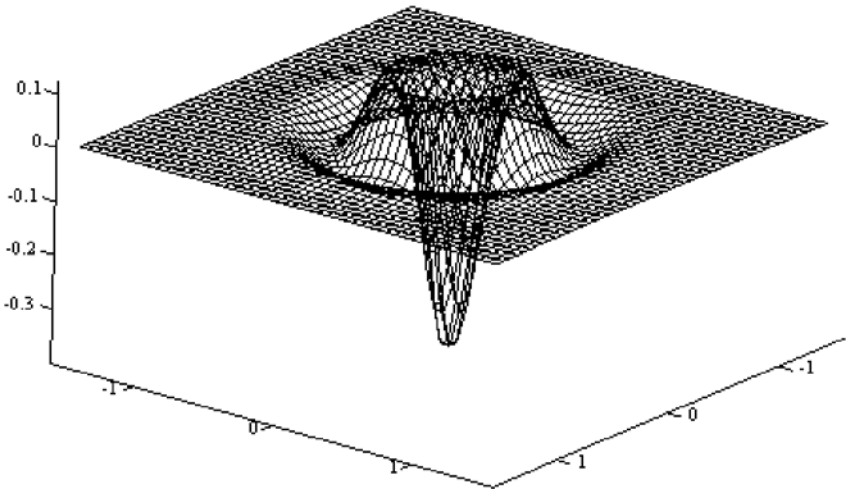

(b)

Fig. 7 The Wigner function as a function of (x, y), where $j = 1, \zeta = 5$, **a** $q = 4$, **b** $q = 5$

odd. The spreading of Wigner over the β-plane is shown as q increases. For the parameter q even, we can see the $W(\beta)$ function is almost positive and has Gaussian central peak. We can see in general when q is even $W(\beta)$ function has upward peak with origin, while it has downward peak when q is odd at the origin. As shown in Fig. 7 the oscillatory behavior is clear for large values of q.

On the other hand, the Q function is positive definite for every point in the phase space. The Q function for a single mode field can be written in a more compact form as

$$Q(\beta) = \frac{1}{\pi}\langle\beta|\hat{\rho}|\beta\rangle \tag{25}$$

where $|\beta\rangle$ is a coherent state. The function $Q(\beta)$ has been constructed in homodyne experiments [47–49]. By considering the properties of Q-function, the interference effects and photon number distribution in phase space can be illustrated [54].

For that purpose we consider the two-mode Q-function in the form

$$Q(\alpha,\beta) = \frac{1}{\pi^2}|\langle\alpha,\beta|\zeta,q\rangle|^2, \tag{26}$$

where $\alpha,\beta\in\mathbb{C}$ and $|\alpha,\beta\rangle = |\alpha\rangle|\beta\rangle$, with $|\alpha\rangle$ and $|\beta\rangle$ the usual coherent states. Generally there are four variables associated with the real and imaginary parts of α,β. For visualization let us confine ourselves to a subspace determined by $\alpha=\beta$ [56]. It is obtained from (24) by written ($s=1$). In that subspace the Q-function for the state (7) is calculated to be

$$Q(x,y) = \frac{\exp[-2(x^2+y^2)]}{\pi^2}\left|N_{q,j}\sum_{n=0}^{q}\frac{\zeta^{2n+j}\alpha^q}{\sqrt{q!}(2n+j)!}\right|^2, \tag{27}$$

where $x=\mathrm{Re}(\alpha)$ and $y=\mathrm{Im}(\alpha)$. We can write the effective function as a function of $r=\sqrt{x^2+y^2}$ on the form $Q(x,y)=A_{q,j}\ f(r)$ where

$$f(r) = r^{2q}\exp[-2r^2]. \tag{28}$$

The maximization or minimization depend on the parameter q. When $q=0$ there exists unique maximum value at $r=0$. For $q>0$ there exists maxima at $r=\sqrt{\frac{q}{2}}$ and minima at $r=0$.

We present in Fig. 8 the function $f(r)$ for different values for q. We find that when $q=0$ the function $Q(r)$ for the state $|\zeta,0\rangle$ has one peak centered at $r=0$, as shown in Fig. 8(a)

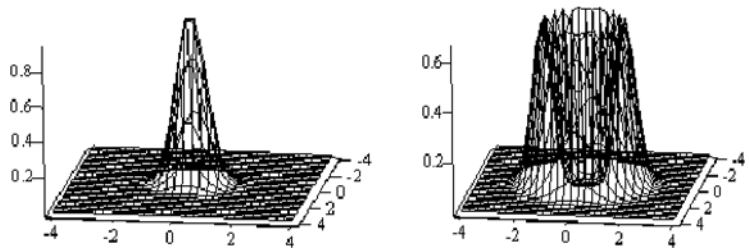

(a) (b)

Fig. 8 The Q-function $Q(x,y)$ as a function of r, **a** $q=0$, **b** $q=5$

and the distribution is almost Gaussian for the vacuum state. For the $|\zeta, 5\rangle$, the shape of the function is sensitive to changes in q (Fig. 8(b)) where the state $|\zeta, q\rangle$ is the most effective state and contribution is the mainly effective one where a crater is apparent in the center. However, if we increase q the crater-like at the center spreads out in the phase space and the diameter increases as the q increases as shown in Fig. 8(b).

6 Conclusion

In this paper we have introduced a new class of nonclassical states, which are referred as superposition of finite dimensional pair coherent states. Mathematically, these states are simultaneous eigenstates of the operator $(\hat{a}^{\dagger}\hat{b} + \frac{\zeta^{q+1}(\hat{a}\hat{b}^{\dagger})^{q}}{(q!)^{2}})^{2}$ and the operators that give the relative occupation numbers of the two modes. Physically, these states can be produced by processes in which there is a strong competition between a two mode parametric conversion. The state appears when the system reaches a stationary regime in the long-time limit of the competition [24, 25]. We have considered some statistical properties of these states. For example, we have considered the Glauber second-order correlation function $g^{(2)}(|\zeta|)$, which shows that the states at $j = 0$ is partially nonclassical for large values of the parameter q with respect to the first mode but for the second is fully nonclassical for a short range of $|\zeta|$ for any values of q. The violation of Cauchy–Schwarz inequalities has been studied in detail. We found the violation depends sensitively on j ($j = 0, 1$), and the parameter q. The phase properties distribution in the Pegg–Barnett approach applied to such states showed that it has a central peak and two wings. We have obtained the formulae for the s-parameterized CF for such state. The interference behavior in phase space for the Wigner function has been shown. Nonclassical signatures for the state (7) have been observed from negativity of Wigner function. Finally the Q-function for some parameters is presented analytically and numerically. We found that both of them are greatly effected with any variation in the parameter q and the parameter ζ.

Acknowledgements I wish to thank Professor A.-S.F. Obada for many valuable discussions of this paper. Also, I am grateful for the helpful comments given by the referees.

References

1. Bloch, I., Köhl, M., Greiner, M., Hansch, T.W., Esslinger, T.: Phys. Rev. Lett. **87**, 030401 (2001)
2. Dalfovo, F., Giorgini, S., Pitaevskii, L., Stringari, S.: Rev. Mod. Phys. **71**, 463 (1999)
3. Leggett, A.J.: Rev. Mod. Phys. **73**, 307 (2001)
4. Chuang, I.L., Nielsen, M.A.: Quantum Computation and Quantum Information. Cambridge University Press, Cambridge (2000)
5. Heiss, D. (ed.): Fundamentals of Quantum Information. Springer, Berlin (2002)
6. Stoler, D.: Phys. Rev. D **4**, 2309 (1971)
7. Yuen, H.P.: Phys. Rev. A **13**, 2226 (1976)
8. Caves, C.M., Schumaker, B.L.: Phys. Rev. A **31**, 3068 (1985)
9. Schumaker, B.L., Caves, C.M.: Phys. Rev. A **31**, 3093 (1985)
10. Glauber, R.J.: Phys. Rev. **131**, 2766 (1963)
11. de Matos Filho, R.L., Vogel, W.: Phys. Rev. A **54**, 4560 (1996)
12. Manko, V.I., Marmo, G., Sudarshan, E.C.G., Zaccaria, F.: Phys. Scr. **55**, 528 (1997)
13. Agarwal, G.S.: J. Opt. Soc. Am. B **5**, 1940 (1988)
14. Agarwal, G.S.: Phys. Rev. Lett. **57**, 827 (1986)
15. Gou, S.-C., Steinbach, J., Knight, P.L.: Phys. Rev. A **54**, 4315 (1996)
16. Diedrich, F., Bergquist, J.C., Itano, W.M., Wineland, D.J.: Phys. Rev. Lett. **62**, 403 (1989)

17. Monroe, C., Meekhof, D.M., King, B.E., Jefferts, S.R., Itano, W.M., Wineland, D.J.: Phys. Rev. Lett. **75**, 4011 (1995)
18. Blockley, C.A., Walls, D.F., Risken, H.: Europhys. Lett. **17**, 509 (1992)
19. Cirac, J.I., Blatt, R., Parkins, A.S., Zoller, P.: Phys. Rev. Lett. **70**, 762 (1993)
20. Cirac, J.I., Blatt, R., Zoller, P.: Phys. Rev. A **49**, R3174 (1994)
21. Cirac, J.I., Parkins, A.S., Blatt, R., Zoller, P.: Phys. Rev. Lett. **70**, 556 (1993)
22. de Matos Filho, R.L., Vogel, W.: Phys. Rev. Lett. **76**, 608 (1996)
23. Meekhof, D.M., Monroe, C., King, B.E., Itano, W.M., Wineland, D.J.: Phys. Rev. Lett. **76**, 1796 (1996)
24. Obada, A.-S.F., Khalil, E.M.: Opt. Commun. **260**, 19 (2006)
25. Khalil, E.M.: J. Phys. A Math. Gen. **39**, 11053 (2006)
26. Yamamoto, Y., Machida, S.: Phys. Rev. A **35**, 5114 (1987)
27. Remoe, G., Schmidt-Kaler, F., Walther, H.: Phys. Rev. Lett. A **293**, 2783 (1990)
28. Loundon, R.: The Quantum Theory of Light. Clarendon, Oxford (1983)
29. Nguyen, B.A., Truong, M.D.: J. Opt. B: Quantum Semiclass. Opt. **4**, 289 (2002)
30. Pegg, D.T., Barnett, S.M.: Eur. Phys. Lett. **6**, 483 (1988)
31. Barnett, S.M., Pegg, D.T.: J. Mod. Opt. **36**, 7 (1989)
32. Pegg, D.T., Barnett, S.M.: Quantum Opt. **2**, 225 (1997)
33. Special issue on Quantum Phase and Phase Dependent Measurements. Phys. Scr. T **48**, 1–142 (1993)
34. Lynch, R.: Phys. Rep. **256**, 367 (1995)
35. Perinova, V., Luks, A., Perina, J.: Phase in Optics. World Scientific, Singapore (1998)
36. Wigner, E.: Phys. Rev. **40**, 749 (1932)
37. Wigner, E.: Z. Phys. Chem. B **19**, 203 (1932)
38. Sudarshan, E.C.G.: Phys. Rev. Lett. **10**, 277 (1963)
39. Husimi, K.: Proc. Phys. Math. Soc. Jpn. **22**, 264 (1940)
40. Kano, Y.: J. Math. Phys. **6**, 1913 (1965)
41. Hillery, M., O'Connell, R.F., Scully, M.O., Wigner, E.P.: Phys. Rep. **106**, 121 (1984) and references therein
42. Lee, H.-W.: Phys. Rep. **259**, 147 (1995)
43. Wünsche, A.: Acta Phys. Slovaca **48**, 385 (1998)
44. Cahill, K.E., Glauber, R.J.: Phys. Rev. **177**, 1857 (1969)
45. Cahill, K.E., Glauber, R.J.: Phys. Rev. **177**, 1882 (1969)
46. Moya-Cessa, N., Knight, P.L.: Phys. Rev. A **48**, 2479 (1993)
47. Leonhardt, U., Paul, H.: Prog. Quant. Electron. **19**, 89 (1995)
48. Leonhardt, U.: Measuring the Quantum State of Light. Cambridge University Press, Cambridge (1997)
49. Schleich, W., Raymer, M. (eds.): Special issues, Quantum State Preparation and Measurement. J. Mod. Opt. **44**(11–12) (1997)
50. El-Orany, F.A.A., Peřina, J.: Opt. Commun. **197**, 363 (2001)
51. Wlodarz, J.J.: Phys. Lett. A **264**, 18 (1999)
52. Richter, Th.: J. Mod. Opt. **48**, 1881 (2001)
53. Wünsche, A.: J. Opt. B: Quantum Semiclass. Opt. **6**, 159 (2004)
54. Mundarain, D.F., Stephany, J.: J. Phys. A Math. Gen. **37**, 3869 (2004)
55. Abramowitz, M., Stegun, I.A.: Handbook of Mathematical Functions with Formulas, Graphs, and Mathematical Tables, 9th edn. Dover, New York (1972)
56. Hyo Seok Yi, Nguyen, B.A., Kim, J.: J. Phys. A Math. Gen. **37**, 11017 (2004)